Studies of Plasma Heated in a Fast-Rising Axial Magnetic Field (Scylla)*

K. Boyer, W. C. Elmore,† E. M. Little, W. E. Quinn, and J. L. Tuck
Los Alamos Scientific Laboratory, University of California, Los Alamos, New Mexico
(Received March 28, 1960)

The Scylla plasma experiment, which employs a rapidly rising magnetic field in a cylindrical mirror geometry to produce and heat a deuterium plasma, is described. Experimental studies of the reproducible neutron emission from the hot plasma show that the neutrons are emitted (1) in a symmetrical, bell-shaped time distribution centered on the maximum of the magnetic field, (2) from a limited region with a 2-cm axial length and a 1.5-cm diameter centered in the compression coil, and (3) in the radial direction with a narrow spread of energies and no significant anisotropy. The time distribution of the neutron emission is shown to be in agreement with a thermonuclear yield curve calculated for an adiabatic compression by the observed magnetic field. The neutron yield has been studied as a function of deuterium pressure, capacitor-bank voltage, and nitrogen impurity. Observations of the space-time distribution of the visible light emission with a streak camera show that (1) a strong radial "shock" occurs at the beginning of the second half-cycle, (2) very little light is emitted from the plasma "fireball" during the time of neutron emission, and (3) an intense luminous flux is produced during the later stages of the discharge. The energy absorbed in each half-cycle of the discharge by the gas is presented as calculated from the incremental damping of the driving magnetic field. Observations of hard x-ray emission (~200 kev) at times of maximum dB/dt for operating pressures in the 5- to 50-micron range are contrasted with the characteristics of the neutron emission in regard to time distribution, pressure, impurities, and rf pre-excitation. Magnetic probe studies of the Scylla discharge are reported and evidence is given that the perturbing effects of the probe dominate the plasma temperature.

INTRODUCTION

ALTHOUGH attempts to produce a laboratory thermonuclear reaction have been prosecuted on a world-wide scale for eight years, there is no authenticated case of such a reaction having been produced as yet by electrical methods. The object of this research was to produce and study a thermonuclear plasma. In this and the accompanying papers, evidence is accumulated in various independent ways that a plasma has been produced with an ion temperature of ~1 kev, an electron temperature of several hundred ev, with a density of $\sim 10^{17}$ deuterons/cc for a duration of ~0.9 μsec. We cannot exclude altogether the possibility that the thermonuclear effects we observe are simulated in some way, but that probability seems to be remote.

The method used to produce the plasma has been proposed in its essentials by many independently, and studied by some, though not duplicated very closely either in physical parameters or experimental behavior. Such studies have been proceeding since 1951, but it is only since August, 1958 (Geneva "Atoms for Peace" Conference) that publication has been unrestricted. Consequently, it is hardly possible to do justice to what has gone before by references from the literature, and we shall therefore attempt to make up for this by slightly fuller references to unpublished work.

The laws of heating by adiabatic compression of a plasma by a magnetic field are well known.[1] The plasma behaves like an ideal gas, which for radial compressions in a time intermediate between the ion-ion collision time and the electron-electron collision time, gives a γ of 2 for the ions and 5/3 for the electrons. All that is needed therefore in principle to reach our desired objective is to produce a low-temperature plasma of temperature T_i confined by a long axial magnetic field of value B_0. Increase of B_0 to B increases T_i to $(B/B_0)T_i$. For this to be true, the compression must be rapid, such that the total probability that an ion shall accumulate a large angle deflection by Coulomb scattering and escape during the compression time τ shall be sufficiently small. In a distribution of energies, the low-energy components will be scattered out preferentially.

An early reference to the production of high temperatures by a combination of shock heating followed by adiabatic compression was due to Wilson.[2] He proposed a rapidly rising barrel-shaped magnetic field, with initial ionization at the outside surface of the gas by electron beams, providing a magnetic implosion. This proposal was circulated and was studied experimentally in Los Alamos by Mather.[3] The magnetic field was produced by two single-turn coils spaced at rather more than one radius apart, placed around a 50-cm diameter glass flask and excited from a 20-kv capacitor bank. Strong convergent shocks were produced which built up in intensity on the first two or three successive oscillations of the exciting current.

Using an apparatus known as Collapse, Colgate *et al.*,[4] performed experiments in which slow radial shocks for preheating were followed by fast radial shocks for further shock heating and adiabatic com-

* This work was performed under the auspices of the U. S. Atomic Energy Commission.
† Present address: Swarthmore College, Swarthmore, Pennsylvania.
[1] R. F. Post, Revs. Modern Phys. 28, 338 (1956).
[2] R. R. Wilson, letter to the U. S. Atomic Energy Commission, 1953 (unpublished).
[3] J. W. Mather, Los Alamos Scientific Laboratory Progress Report, October, 1953 (unpublished); Washington Report Wash-184, October, 1954 (unpublished), p. 51.
[4] S. A. Colgate, Conference on Thermonuclear Reactions [Washington Report Wash-289, June, 1955 (unpublished), p. 176]. S. A. Colgate and R. E. Wright, *Proceedings of the Second United Nations International Conference on the Peaceful Uses of Atomic Energy, Geneva, 1958* (United Nations, Geneva, 1958), Vol. 32, p. 145.

pression. Concurrent with this was the work on axial shocks at Los Alamos by Scott *et al.*[5] These shocks were launched at the ends of cylindrical tubes either by small axial compressions or by conical pinches.[6] In an experiment known as Totempole,[7] the increase of temperature produced by colliding these shocks at the midpoint of the tube was followed by a radial compression in a rising axial magnetic field. Next we have the extensive studies of Kolb *et al.* at the Naval Research Laboratory.[8] These initially used axial shocks projected from a T tube, followed by compression in a rising axial magnetic field. The concept of confinement in a mirror geometry with axial-field compression is discussed in a theoretical paper by Terletski.[9] A recent manifestation of the same axial-field compression geometry known as the Thetatron[10] is reported from the United Kingdom. In low-power experiments, compression and confinement were observed in a uniform axial increasing magnetic field, and a toroidal version is under construction. Various other axial magnetic field compression devices with mirrors are now being studied in many parts of the world (see note at end of paper).

From the studies with Totempole,[7] it became clear that thermonuclear temperatures could not be attained in that apparatus. The magnetic field rose to its maximum value of 60 kilogauss in 10 to 20 μsec. At this rate of compression, there is time enough for significant escape of heated plasma from the compression region. The relation between loss probability and compression time takes a simple form for purely radial fast compressions with negligible electron pressure. The probability P of scattering per unit time is given by $n\sigma v$, which with appropriate cutoff procedure for the integration over the Coulomb scattering, amounts to $n(2.6\times10^{10}W^{\frac{3}{2}})^{-1}$ sec^{-1}, where n is the number of deuterons per cm^3, and W is the deuteron energy in kev. For a purely radial compression $n/n_0=B/B_0=W/W_0$, where the subscript denotes the initial condition.

Let the magnetic field increase from B_0 to B linearly in time τ; then $W=W_0[1+(\alpha-1)t/\tau]$, and $n=n_0\times[1+(\alpha-1)t/\tau]$, where $\alpha=n/n_0$. The scattering probability is given by

$$P=\int_0^\tau \frac{n(t)dt}{2.6\times10^{10}[W(t)]^{\frac{3}{2}}}$$
$$=\frac{1}{1.3\times10^{10}}\frac{n_0}{W_0^{\frac{3}{2}}}\frac{(\alpha^{\frac{1}{2}}-1)}{\alpha-1}\tau. \quad (1)$$

For unit scattering probability, normalizing to a final temperature of one kilovolt, we find:

With $n_0\simeq10^{15}$, $W_0=0.1$ kev, $\alpha=10$, $\tau=1.6$ μsec.
$W_0=0.1$ kev, $\alpha=100$, $\tau=4.4$ μsec.

For a purely two-dimensional compression, these considerations apply, even to the case of a high-density plasma, for which $B^2/8\pi$ outside equals nkT in the plasma, such as would occur for compression in a mirror geometry where the length is much greater than the diameter. For a short mirror geometry, the axial compression introduces heating in the axial direction and it turns out that a different criterion for confinement arises. For confinement at unit β, $(=8\pi\, nkT/B^2)$[11] in a plasma with a transition region between plasma and compressing field of thickness δ [given by the Rosenbluth and Garwin relation[12] $\delta=(mc^2/8\pi n_0e^2)^{\frac{1}{2}}$], the mean plasma half-life has been given by Grad,[13]

$$\tau\approx10^{-6}BR^2/T, \quad (2)$$

where B is the magnetic field in gauss, T is the plasma temperature in ev, and R is the characteristic size of the confined plasma. Now from an examination of the peak heated region (fireball), it turns out that the compression is fairly closely equal in each dimension, 3.6 in the radial direction and 3.5 in the axial direction. Consequently, the criterion given above is the more closely applicable. To evaluate T in the most pessimistic way, we shall take the final values $B_f=60$ kilogauss, $T_f=1000$ ev, and $R=0.5$ cm, giving $\tau=15$ μsec. According to this, from the plasma confinement point of view, a slower compression than that indicated by Eq. (1) could be used.

The choice of the magnetic field configuration at the ends of an axial magnetic compression device involves a compromise. A uniform axial magnetic field, falling at the ends, has neutral stability but no end confinement. Introduction of mirrors gives partial confinement, but if the magnetic lines are not anchored on conductors (which does not seem to be possible in fast transient devices) mirror machines are believed subject to hydromagnetic flute instability at high values of β. Uniform compression in a torus disposes of axial losses

[5] Scott, Basmann, E. M. Little, and D. B. Thomson, *The Plasma in a Magnetic Field* (Stanford University Press, Palo Alto, California, 1958), p. 110.
[6] V. Josephson, J. Appl. Phys. **29**, 30 (1958).
[7] E. M. Little and D. B. Thomson, Los Alamos Scientific Laboratory Progress Report, June, 1957 (unpublished); Los Alamos Scientific Laboratory Report LA-2202, 1958 (unpublished).
[8] A. C. Kolb, Bull. Am. Phys. Soc. **2**, 47 (1957); Phys. Rev. **107**, 345 (1957); *Proceedings of the Second United Nations International Conference on the Peaceful Uses of Atomic Energy, Geneva, 1958* (United Nations, Geneva, 1958), Vol. 31, p. 328.
[9] T. P. Terletski, J. Exptl. Theoret. Phys. (U.S.S.R.) **32**, 927 (1957) [translation: Soviet Phys.-JETP **5**, 755 (1957)].
[10] Gatlinburg Conference on Theoretical Physics of Controlled Thermonuclear Reactions, April, 1959 [Atomic Energy Commission Report TID-7582 (unpublished)], p. 26.
[11] C. L. Longmire and M. N. Rosenbluth, Ann. Phys. **1**, 120 (1957).
[12] M. Rosenbluth and R. Garwin, Los Alamos Scientific Laboratory Report LA-1850, 1955 (unpublished).
[13] H. Grad, New York University Report NYO-7969, 1957 (unpublished).

but the system then is subject to hydromagnetic interchange instability and gross drift to the walls. Both of these can of course in principle be disposed of by the introduction of a rotational transform.[14]

FIRST SCYLLA DEVICE

From observations on shock velocities produced in deuterium it was believed that plasma temperatures in the region of 100 ev could be produced behind the shock. The above analysis indicated that it should be possible adiabatically to compress the plasma to a density and temperature such that a detectable thermonuclear reaction could be observed. An experiment was devised to use an oscillating mirror field to ionize, shock heat, and adiabatically compress a deuterium plasma starting with a weakly ionized gas having a density of 10^{15} deuterons per cm^3. The first Scylla device[15] as described below was designed from the following considerations within the limitations of the components available.

The fraction of deuterons confined by the magnetic field at peak compression and the initial temperature as determined by the strength of the shock should both be proportional in some manner to the time rate of change of the magnetic field B at the beginning of the cycle, so that it is desired to maximize this quantity. For a single-turn solenoid, dB/dt is given approximately by the relation

$$\frac{dB}{dt}=\frac{10^8V}{\pi R^2(1+\lambda)}, \tag{3}$$

where B is the magnetic field in gauss, V is the capacitor potential in volts, λ is the ratio of the parasitic inductance to the coil inductance, and R is the coil radius in cm. However, the particle pressure, nkT, which should be as large as possible, must be balanced by the magnetic pressure, $B^2/8\pi$. The magnetic energy in the coil is given by the integral of the magnetic pressure over the coil volume and shares the capacitor bank energy $\frac{1}{2}CV^2$ with the parasitic inductance so that

$$B^2=\frac{4\times10^7CV^2}{R^2l(1+\lambda)}, \tag{4}$$

where C is the bank capacity in farads and l is the coil length in cm. The product B^2dB/dt is therefore a figure of merit for the system and is given by

$$B^2\frac{dB}{dt}=\frac{4\times10^{15}CV^3}{\pi R^4l(1+\lambda)^2}. \tag{5}$$

This shows that the capacitor bank voltage, the capacity, the coil radius, and the leakage inductance are all sensitive parameters. While decreasing the coil length improves the nkT product, it decreases the volume and increases the relative leak rate so that its effect on the system is less clear. However, a longer coil makes the ratio λ more unfavorable. The initial Scylla was constructed using two banks of five 100-kv capacitors[16] ($C=0.87\ \mu$f, $L\simeq0.1\ \mu$h) placed in parallel and connected through three-element triggered spark gaps to single-turn coils surrounding a 5-cm internal diameter Pyrex tube. The coils consisted of copper bands, 0.63 cm thick and 2.5 cm wide, and were spaced a distance equal to the mean coil diameter of 7.0 cm. All connections were made with flat copper-sheet transmission lines insulated with polyethylene sheet to minimize parasitic inductance. Each coil proved to have an inductance of 0.08 μh, each capacitor bank and gap an inductance of 0.13 μh, so that 39% of the capacitor voltage appeared initially across the coils. With the banks charged to 65 kv, a limit set by external spark breakdown, a peak central compression field of about 38 kilogauss was obtained 1.5 μsec after the spark gaps were triggered. The field then continued as a damped oscillation.

In this and subsequent experiments, a continuous flow of deuterium gas was maintained through the discharge tube. Operating pressures in the 10- to 1000-micron range were measured using a Pirani gauge calibrated for deuterium. With no gas flow the base vacuum pressure usually reached a value of $\lesssim10^{-6}$ mm Hg. In all experiments with Scylla the deuterium gas was partially preionized by applying 1 kw of 27.1-Mc/sec radio-frequency power to insulated wires surrounding the tube on each side of the coil arrangement.

The device described produced bursts of about 10^4 neutrons, as well as hard x rays at the lower pressures. It was found that a discrepancy in timing of the two spark gaps of 0.2 μsec considerably reduced the neutron yield, and the yield disappeared when the time discrepancy reached 0.5 μsec. These observations served principally to emphasize the importance of plasma containment. The ability of the device to produce neutrons, together with other encouraging results that have since been studied in more detail, led to the design of an improved version of Scylla.

SECOND SCYLLA DEVICE

The principal results reported here and in the following papers[17,18] were obtained with the second Scylla device as described below. The important changes in design are the following: (1) To minimize the effect of spark-gap inductance each of the ten 100-kv capacitors

[14] L. Spitzer, Phys. Fluids **1**, 253 (1958).

[15] W. C. Elmore, E. M. Little, and W. E. Quinn, Proceedings of the Controlled Thermonuclear Conference [Atomic Energy Commission Report TID-7553, February 3, 1958 (unpublished)]; Phys. Rev. Letters **1**, 32 (1958). W. C. Elmore, E. M. Little, W. E. Quinn, and K. Boyer, *Proceedings of the Second International Conference on the Peaceful Uses of Atomic Energy, Geneva, 1958* (United Nations, Geneva, 1958), Vol. 32, p. 337.

[16] Tobe Deutschmann Corporation, Norwood, Massachusetts.

[17] F. C. Jahoda, E. M. Little, W. E. Quinn, G. A. Sawyer, and T. F. Stratton, following paper [Phys. Rev. **119**, 843 (1960)].

[18] D. E. Nagle, W. E. Quinn, F. L. Ribe, and W. B. Riesenfeld, this issue [Phys. Rev. **119**, 857 (1960)].

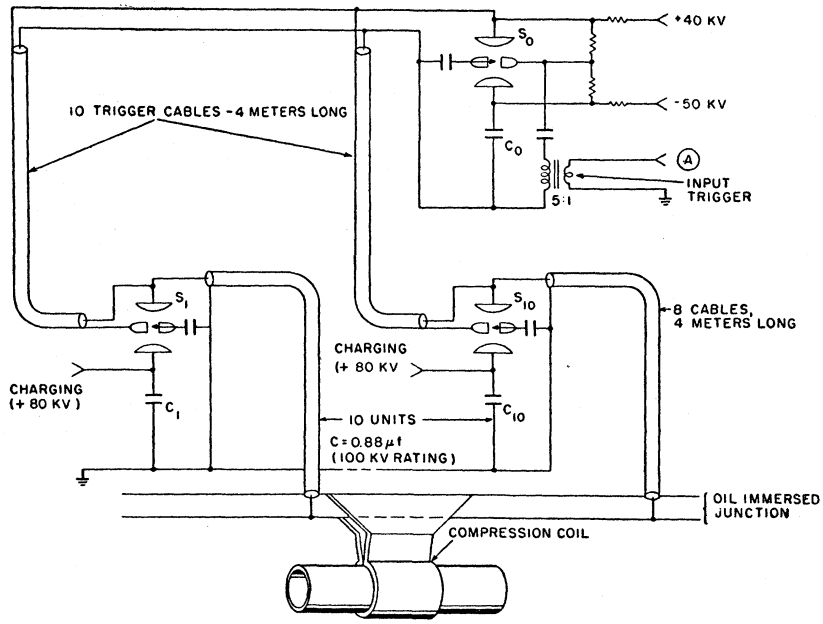

FIG. 1. Electrical schematic circuit diagram of Scylla.

is supplied with a four-element triggered spark gap.[19] The ten gaps are connected in parallel with cables to a single compression coil. (2) A method was developed for triggering all ten gaps within 0.04 μsec. (3) The ten capacitors are charged dynamically in a time of 50 μsec from a five-stage cascade capacitor bank (Marx circuit). This avoids difficulties with high dc potentials and increases the capacitor life. (4) The two separated, single-turn coils were replaced by a single, shaped coil having greater efficiency in establishing the desired axial magnetic field within the active region of the discharge tube. (5) Improvements have been made in the choice of discharge tube material. Since the development of the power source (Fig. 1) to drive the compression coil was a major problem in attaining a workable device, this system is described in detail in the Appendix.

The shaped single-turn coil whose section is shown in Fig. 2 led to an order of magnitude increase in the neutron yield. The magnetic field lines cannot penetrate the coil walls in the time of the experiment so that they define magnetic flux surfaces. The field distribution within the coil, its mirror ratio, and its approximate inductance are easily found using an analog computer.[20] A limited series of different coil shapes were studied to find the one that maximizes neutron yield at a fixed operating potential. Data relating the coil shapes studied to relative neutron yield, with Scylla operating at 70 kv and 100-microns pressure are summarized in Table I. Coil A appears to have the most favorable shape of those tried. In addition, a few observations were made with a tube and coil 50% smaller in diameter, and with a tube and coil 38% larger in diameter, with a marked falling off in neutron yield in both cases. It should be appreciated that these variations were limited by the necessity of retaining a ceramic tube of uniform diameter so that high mirror ratios result in lower compression fields. The scaling laws for axial compression devices show that the thermonuclear yield is favored for constant energy in the B field by going to minimum size. However, there is a limit to the smallness set by the following two factors: (1) the constant parasitic inductance of the power supply eventually dominates the total inductance, and (2) the closer proximity of the walls increases the influx of impurities to the heated region.

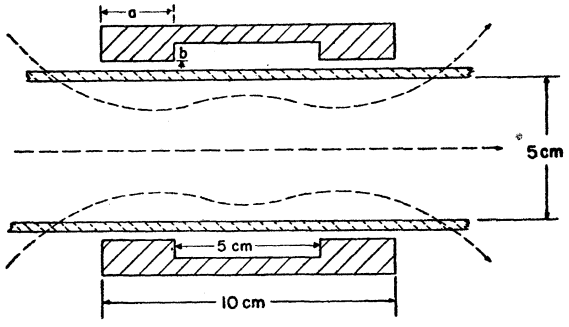

FIG. 2. Axial cross section of Scylla compression coil.

All the results described in subsequent sections were obtained either with coil A, or with a similar coil A' made eight percent larger in order to fit a commercial size of alumina tubing. Coil A' has an inductance of 0.038 μh so that 49% of the capacitor voltage V appears across the coil terminals. The peak current is $10.6V$

[19] R. S. Dike, D. W. Lier, A. E. Schofield, and J. L. Tuck (to be published).

[20] K. E. Wakefield, Project Matterhorn Report NYO-7313, December 13, 1956 (unpublished).

amperes and the peak central compression field, in the absence of plasma, is $0.71V$ gauss. The period of oscillation with no gas is 5.17 μsec, and with deuterium at 90-μ pressure it is .5.0 μsec. The time for compression, of course, is one-quarter period. The Q of the oscillation with no gas is 15, indicating that the equivalent series damping resistance is 6.3 milliohms. The present Scylla is regularly operated with capacitor voltages as high as 90 kv.

The discharge tube walls undergo rather severe treatment, since approximately 50% of the capacitor bank energy is ultimately deposited at the walls via radiation and particle wall collisions as the externally applied magnetic field is sinusoidally damped. The discharge tube originally used was a heavy-walled Pyrex glass tube. After a few firings it became heavily crazed and discolored. Vycor and fused quartz, which also become heavily crazed, are only slightly better, lasting at most 30 discharges. The neutron yield from the Pyrex and Vycor tubes is low and erratic. However, a transparent tube is needed if one wishes to observe plasma motion from the side.

TABLE I. Neutron yield versus coil shape.

Coil	Coil dimensions a (cm)	b (cm)	Relative neutron yield (%)
A	2.54	0.64	100
B	0.64	0.64	11
C	1.59	0.64	62
D	3.80	0.64	30
E	3.10	0.64	80
F	1.90	1.27	59
G	10.57	0	10

Ceramic tubes have proved to last longer and give higher neutron yields. Much early work was done with a Mullite combustion tube.[21] Tubes of this material containing 60% alumina require as many as fifty discharges before a high but erratic neutron yield is obtained. This behavior is attributable to the gradual removal of volatile impurities from the wall. The most satisfactory wall material used to date is 96% vitreous alumina.[22] With this material high and reproducible neutron yields are obtained after only a few firings. One such tube lasted for 3400 discharges, its wall having eroded from an initial thickness of 0.3 cm to a thickness of 0.1 cm in the discharge region at the time of breaking. Figure 3 shows this tube cut in sections together with a compression coil. Much of the wall material that erodes away either deposits as a black material on each side of the active discharge region, or collects as a sand-like material at the far ends of the tube.

[21] McDaniels Refractory Porcelain Company, Beaver Falls, Pennsylvania.

[22] Coors Porcelain Company, Golden, Colorado.

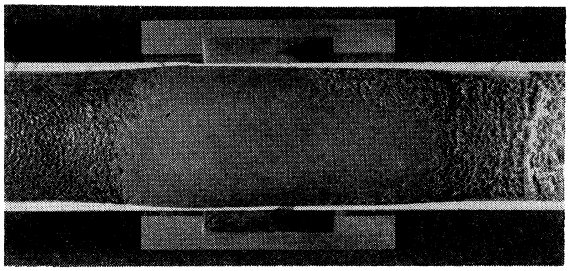

FIG. 3. Sections of 96% alumina tube after 3400 discharges and a Scylla coil.

VISIBLE LIGHT EMISSION

Visible light seen through a Pyrex end window has been studied both with a telescope coupled to a photomultiplier tube to detect the time variation of average light intensity, and with a fast moving-image camera, to study its space-time distribution. Light seen by the telescope focussed on a 3-cm diameter region at the center of the coil varies in intensity over a considerable range. The data, summarized in Fig. 4, required several discharges to cover the complete range of intensities. This record shows that negligible light emission occurs until after the first field reversal. During the second half-cycle the light intensity grows rapidly. Similar steps in intensity occur during the next three half-cycles, with maximum intensity coming at the end of the fifth half-cycle. This behavior will now be correlated with observations made with the moving-image camera, and with a calculation of the rate at which the gas discharge absorbs energy from the oscillating magnetic field.

The moving-image camera which was used has a nominal $f/4.5$ (measured $f/7.5$) aperture and a maximum writing speed on the film of 5 mm/μsec. A blast shutter[23] was used to terminate the period of recording in order to eliminate rewriting on the film and to eliminate scattered light arising after the desired time interval has been recorded. The 0.15-mm slit of the camera was focussed on the central tube diameter through the end window so as to obtain a time-resolved

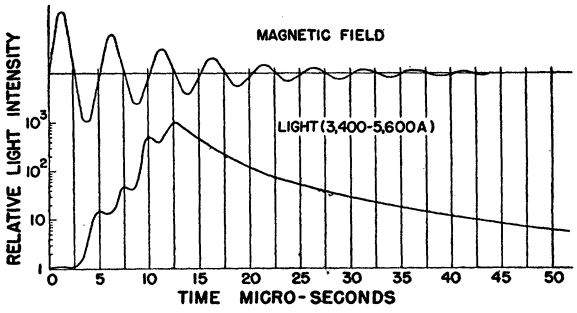

FIG. 4. Intensity of visible light emission from Scylla as a function of time.

[23] Berlyn Brixner, J. Soc. Motion Picture Engrs. **59**, 503 (1952).

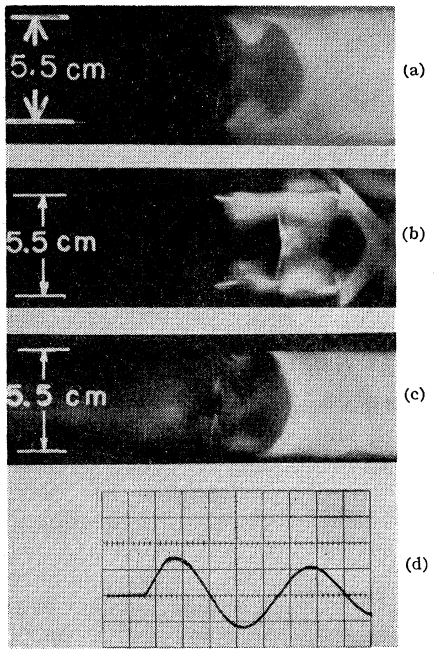

FIG. 5. Streak photographs of the radial motion of the light emitting portions of the plasma in the coil midplane. (a) and (b) Deuterium gas at a pressure of 90 μ with a capacitor bank voltage of 84 kv. (c) Helium gas at a pressure of 115 μ and a capacitor bank voltage of 84 kv. (d) Applied magnetic field which sets the time scale, 1 μsec per division.

record of the radial motion of the light-emitting portions of the plasma in this region. Figures 5(a) and 5(b) were taken with deuterium gas at a pressure of 90 μ, a bank voltage of 84 kv, with a neutron yield of 7×10^6. Figure 5(c) was taken with helium gas at a somewhat higher pressure and shows the shock fronts more clearly. Figure 5(d) shows a current trace on the same time scale as that of the moving image photographs. In the case of Fig. 5(a) the discharge was contaminated because of the presence of metal rings on either side of the compression coil. The impurity radiation in this case gives a more intense image and better illustrates the plasma structure at the beginning of the second half-cycle.

Examination of Fig. 5 reveals a pulse of light throughout the tube occurring at the start of the first half-cycle with no evidence of a shock wave. Negligible light is emitted during the remainder of this half-cycle. Just at the first field reversal, a thin luminosity travels radially inward with a velocity of 15 cm/μsec. In the case of the helium record this luminosity shows more clearly, and it is reflected from the central region. During the second half-cycle very little light comes from the central compressed region, but light from wall impurities moves inward and then outward with the applied magnetic field as the second half-cycle progresses. A slower (5 cm/μsec) brighter luminosity initiates the third half-cycle, and impurity light now comes from the central region showing the presence of some impurity atoms throughout the plasma. The record is terminated in Fig. 5(b) by the blast shutter. Other records lasting for a longer time show an even greater rise in impurity light during the fourth and fifth half-cycles.

It is now clear that most of the features of the gross light intensity record of Fig. 4 are due to light arising from impurities gradually contaminating all of the plasma during successive oscillations of the field. The presence of increasing amounts of impurities appears also to affect the rate of energy absorption by the plasma. The energy absorbed in each half-cycle was estimated from oscilloscope traces of the oscillating external magnetic field. With no gas present the amplitude decreases exponentially with a logarithmic decrement of 0.209 ($Q=15$). The energy dissipated in the gas per half-cycle computed in the above way is shown in Fig. 6, where unity relative energy input corresponds to 3900 joules per half-cycle. The energy dissipated in the first and second half-cycles is small, rising to a maximum in the third, fourth, and fifth half-cycles. This is clearly correlated with the visible light intensity curve. Impurities evidently increase the plasma resistance, changing the discharge from one that is primarily inductive in the second and possibly the third half-cycle, to one that is primarily resistive in subsequent half-cycles.

NEUTRON EMISSION

Neutron emission from Scylla has been detected with a lead-shielded plastic scintillator for time-history studies, and with silver foils for measuring absolute yields. The silver detector contains four Geiger tubes

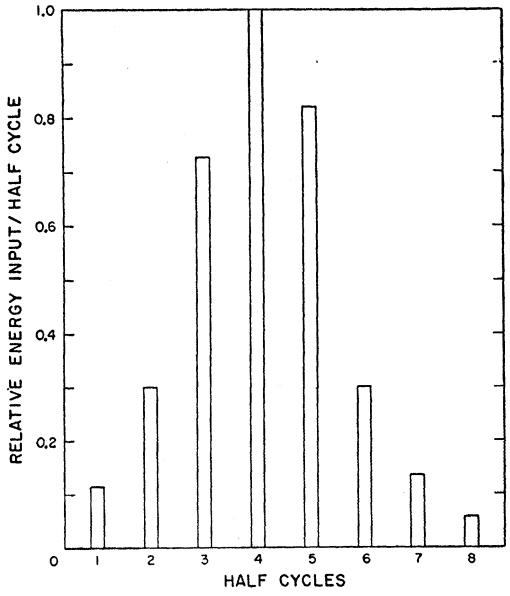

FIG. 6. Energy dissipated in the gas per half-cycle where unit relative energy input corresponds to 3900 joules per half-cycle.

surrounded by 10-mil silver foil, imbedded in a paraffin block 30×30×15 cm that is shielded for slow neutrons by 30-mil cadmium sheet. Calibration of this detector with *d-d* neutrons from a Cockcroft-Walton generator indicates that each count in a one-minute counting period corresponds to 3000 neutrons from a point source at the distance used with Scylla. This type of silver counter[24] was developed as a secondary standard for absolute measurement of neutron fluxes over a wide range of intensity.

The typical time distribution of neutrons from Scylla is shown in Fig. 7(a) (lower trace) by the oscilloscope trace of the photomultiplier current arising from proton recoils in the lead-shielded plastic scintillator. The rise-time of the detecting-recording system is less than 0.1 μsec so that the trace is an accurate record of the neutron production rate. The other trace presents the magnetic field of the coil as given by the integrated signal from an electrostatically shielded one-turn pick-up loop mounted above the compression coil. A careful study of this, and many other similar records for a variety of operating conditions, indicates that neutrons occur in bell-shaped, symmetrical bursts, centered on the second, third, and sometimes later, magnetic field maxima and having a 0.9-μsec width at half-height. At low pressures very small bursts are observed at the fourth and fifth maxima (see Fig. 14), but no neutron emission was observed in the first half-cycle in these experiments.

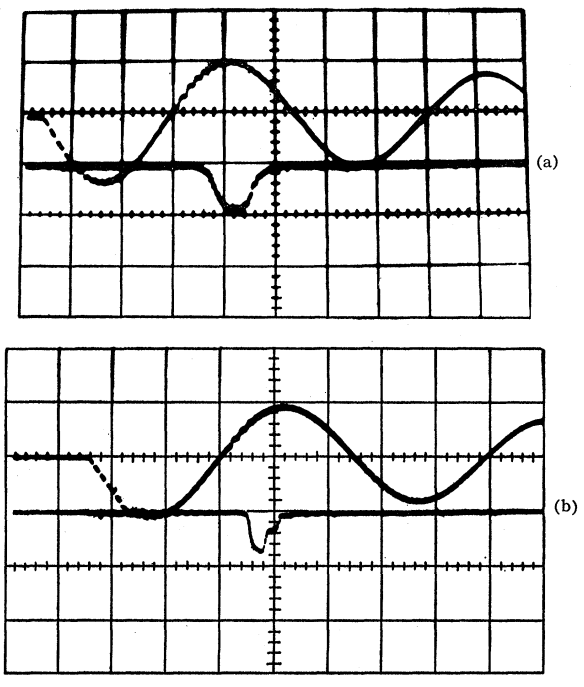

FIG. 7. (a) The time distribution of neutron emission (lower trace) in mirror coil *A* with the applied magnetic field (upper trace). The time scale is 1 μsec per division. (b) The time distribution of neutron emission (lower trace) in mirrorless coil *G* with the applied magnetic field (upper trace). The time scale is 1 μsec per division.

[24] D. E. Bannerman and H. J. Karr, Los Alamos Scientific Laboratory (private communication).

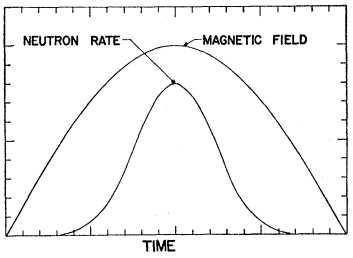

FIG. 8. The theoretical time distribution of the neutron production rate calculated for $\gamma = 5/3$ assuming a simple adiabatic compression and a temperature of 1 kev at peak magnetic field.

Figure 8 shows a theoretical curve of neutron production rate R calculated for $\gamma = 5/3$, assuming a simple adiabatic compression model for which the following equations apply:

$$PV^{\gamma} = \text{constant}; \quad P = \beta B^2/8\pi; \quad PV = 2NkT, \tag{6}$$

$$R = \tfrac{1}{2}(N/V)^2 V\langle\sigma v\rangle, \tag{7}$$

where $\langle\sigma v\rangle$ is the Maxwell-Boltzman average of σv for a temperature T, and N is the total number of deuterons. The temperature at peak magnetic field was assumed to be 1 kev. The shape of the neutron curve is rather insensitive to the assumed value of the maximum temperature. The width of the curve at half-maximum and its general shape agree quite well with observed curves of the neutron production rate [see Fig. 7(a)].

An exception to the coincidence of the neutron and magnetic peaks is found with coil G which produces a nearly uniform axial field offering no mirror containment. The neutron intensity shown in Fig. 7(b), rises in the usual way but breaks sharply at 0.4 μsec and falls to zero at the time of peak compression, giving approximately 10% of the normal shaped-coil yield.

The dependence of total neutron yield on deuterium pressure is shown in Fig. 9. These data were taken with the capacitor bank charged to 84 kilovolts. The decrease in neutron yield at the lower pressures may result from decreased ionization efficiency as evidenced by the time shift of the major neutron emission from the second to the third magnetic compression. The decrease in neutron yield at the higher pressures may arise from the fact that at constant nkT, the thermonuclear yield falls with increasing n in this temperature range.

In Fig. 10, the total neutron yield is shown as a function of capacitor bank voltage at a deuterium pressure of 90 microns. The dependence of total neutron yield on nitrogen impurity present in the deuterium gas is shown in Fig. 11. These observations were made with the capacitor bank charged to 84 kv and with a deuterium pressure of 90 microns. The reduced neutron yield is expected since the admixture of a higher Z impurity gas rapidly increases the competing radiation losses from the plasma.

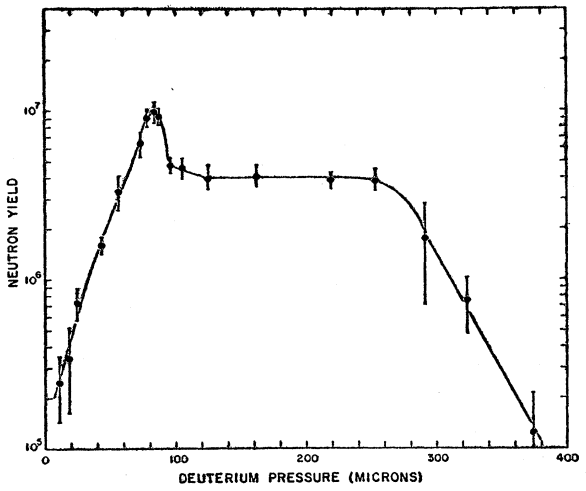

FIG. 9. The neutron yield as a function of deuterium pressure with a capacitor bank voltage of 84 kv.

The location, size, and shape of the neutron emitting source or "fireball" have been established with a massive neutron collimator made from paraffin loaded with lithium to absorb neutrons without γ-ray emission. The neutron collimator had cylindrical symmetry with; an aperture diameter of 1 cm, a 56-cm collimation length, an outside diameter of 40 cm, and an over-all length of 82 cm. In order to reduce the neutron scattering for these measurements and for the neutron energy experiment to be described next, the metal of the compression coil was reduced to a thickness of 0.3 cm by machining material from the outside of the coil. Fast neutrons from the source perpendicular to a plane through its axis pass through the 1-cm diameter cylindrical aperture to a lead-shielded plastic scintillator and fourteen-stage photomultiplier coupled to a cathode-ray oscilloscope. Pulses recorded for various positions of the collimator are corrected for background and normalized against the total yield indicated by the silver counter. The data obtained at a deuterium pressure of about 100 μ and an operating voltage of 84 kv are presented in Fig. 12, which indicates the source to be a well-defined region approximately 1.5 cm in diameter and 2 cm long centered in the compression coil. In these graphs a small correction has been made for the size of the collimator aperture. The neutrons clearly originate in the plasma away from the tube walls and in the region of mirror confinement, where both radial and axial compression have occurred. In the radial direction, the neutron emitting region is shifted away from the coil axis toward the feedpoint gap. This is in excellent agreement with the weakening of the field produced by the current leads to the coil and the similar displacement observed in the soft x-ray emitting region as discussed in a later paper.[17]

One of the most important questions is whether the observed neutrons are of thermonuclear origin or are the result of collisions between a cold plasma and a small group of deuterons which have acquired large kinetic energies by some mechanism which is irrelevant to the temperature of the plasma. If it can be shown that the neutrons originate from fusion reactions in the deuterium plasma with random thermal motion, then neutron measurements provide a sensitive method of measuring plasma temperatures as well as yielding information on plasma density and position. A powerful method that has been used to determine the origin of neutrons from linear[25] and toroidal[26,27] pinch devices involves measuring their energy spectrum by scanning proton recoils in nuclear emulsions or cloud chambers

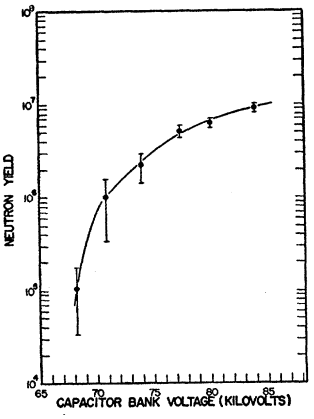

FIG. 10. The dependence of neutron yield on capacitor bank voltage with a deuterium pressure of 90 μ.

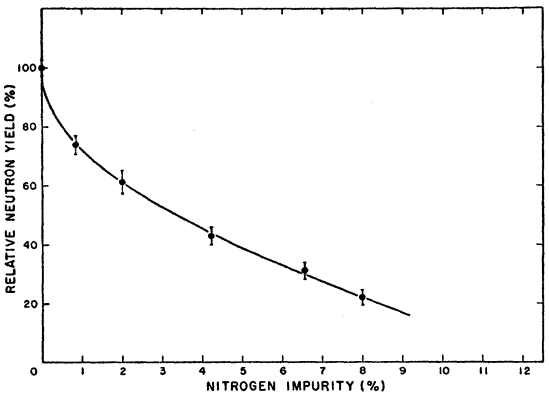

FIG. 11. The neutron yield as a function of nitrogen impurity with a deuterium pressure of 90 μ and with a capacitor bank voltage of 84 kv.

[25] J. W. Mather and A. H. Williams, *Proceedings of the Second United Nations International Conference on the Peaceful Uses of Atomic Energy, Geneva, 1958* (United Nations, Geneva, 1958), Vol. 32, p. 26.

[26] J. P. Conner, D. C. Hagerman, J. L. Honsaker, H. J. Karr, J. P. Mize, J. E. Osher, J. A. Phillips, and E. J. Stovall, Jr., *Proceedings of the Second United Nations International Conference on the Peaceful Uses of Atomic Energy, Geneva, 1958* (United Nations, Geneva, 1958), Vol. 32, p. 297.

[27] G. N. Harding, A. N. Dellis, A. Gibson, B. Jones, D. J. Lees, R. W. P. McWhirter, J. A. Ramsden, and S. Ward, *Proceedings of the Second United Nations International Conference on the Peaceful Uses of Atomic Energy, Geneva, 1958* (United Nations, Geneva, 1958), Vol. 32, p. 365.

as detectors. Tests of this sort with pinches have all revealed large anisotropies of the mean neutron energy, showing that the neutrons have arisen from acceleration processes rather than from high plasma ion temperatures. In order to test for such energy shifts in pinch devices, one looks for energy differences of neutrons leaving the pinch region tangentially parallel and antiparallel to the direction of the ion current. To look for such a tangential energy shift in Scylla requires shielding a portion of the source above a plane parallel to its axis while recording neutrons from the unshielded part. In practice it is convenient to detect neutrons from the upper third of the fireball, and to reverse the magnetic field direction in the coil to simulate the lower third. Such a test should reveal whether or not the neutrons

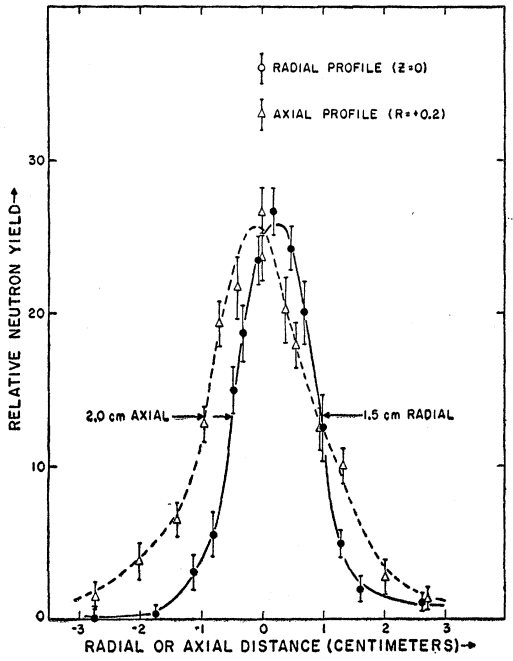

FIG. 12. Relative neutron intensity from Scylla along the radial and axial directions.

are produced by deuterons having a rotational velocity about the axis.

For this test a thick flat paraffin plate was mounted with its upper surface 0.33 cm above a plane passing through the axis of the compression coil. Six one-hundred micron nuclear emulsions (Ilford *C*-2) were placed 15 cm and 20 cm from the axis. Scylla was then operated 1000 times, with a yield of several million neutrons per discharge for each direction of its magnetic field. Data read from the two sets of plates, shown in Fig. 13, demonstrate that the average neutron energy shifts by a small amount, estimated to be 22 kev, when the magnetic field is reversed. Expressed in terms of the rotational energy of the deuteron according to the model discussed below this amounts to a very small

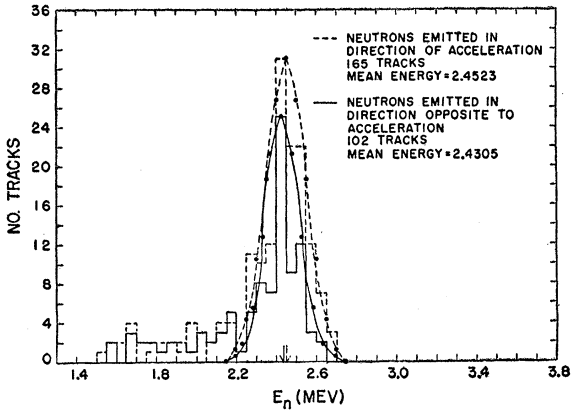

FIG. 13. Neutron energy spectrum from Scylla for the two polarities of the applied voltage.

deuteron energy of 60 ev. That this drift is real, however, is indicated by a statistical analysis which gives it a probability of 0.99. It can be argued that since there is necessarily a gradient of the magnetic field between the outside of the plasma and its interior, the rotational velocity produced in the surface layer, given by $cmv_\perp^2\mathbf{B}\times\nabla\mathbf{B}/2eB^2$, is of this order of magnitude. Similarly the rotation could be caused by an $\mathbf{E}\times\mathbf{B}/B^2$ drift from a radial electric field. For comparison, the anisotropy in pinch experiments may amount to 1000 times this value.

To relate the shift in average neutron energy with field reversal to average deuteron motion in the direction of observation requires some sort of model. For example, if one assumes that all particles rotate with uniform angular velocity about the axis of the coil, the average neutron energy shift is

$$\Delta E_n = 2m_n v_0 v_c \langle (r/a)\sin\theta\rangle, \tag{8}$$

where m_n is the neutron mass, v_0 is the velocity with which a *d-d* neutron is emitted in the center-of-mass system, v_c the peripheral velocity of the rotating plasma (assumed to be a cylinder of radius a), and r and θ are coordinates of a point in the cylinder. The energy of a peripheral deuteron is then

$$W_d = \tfrac{1}{2}(2m_n)v_c^2 = (\Delta E_n)^2/8E_0 f^2, \tag{9}$$

where $E_0=\frac{1}{2}m_n v_0^2=2.45$ Mev, and $f=\langle(r/a)\sin\theta\rangle$, with the average taken over the portion of the plasma cylinder between the plane of the paraffin shadow bar, and the outer radius (0.75 cm) of the cylinder. A calculation shows that for this model $f^2\approx 0.4$, and W_d is approximately 60 ev. This sample calculation serves to demonstrate the exceedingly small center-of-mass deuteron motion necessary to account for the observed shift in average neutron energy. The energy shift is too low by more than a factor of 10 to have an appreciable effect on the observed *d-d* reaction rate.

The neutron energy distributions of Fig. 13, in addition to showing the small energy shift discussed above,

TABLE II. Inferred ion temperature (kev) from the widths of the neutron energy curves.

Curve	σ_{uncor}	σ_{instr}	σ_{cor}	kT
Solid (1)	86.4	80.0	32.7	0.9±0.9
Dashed (2)	100.4	80.0	60.6	3.0±1.5
	$\langle\sigma^2\rangle^{\frac{1}{2}}=\left[\frac{(\sigma_{\text{cor}})_1^2+(\sigma_{\text{cor}})_2^2}{2}\right]^{\frac{1}{2}}$		=48.7	1.9±1.2

also show appreciable widths. It is instructive to determine the ion temperature to which these widths might correspond if they were due to thermal broadening of the neutron energy spectra because of random motions of the reactant deuterons in a Maxwellian distribution. The result, though necessarily crude, can be compared with that determined much more precisely in a later experiment[18] on the thermal broadening of the proton and triton energy spectra from the *d-d* reaction. It is shown in reference 18 that the standard deviation of the neutron energy distribution would then be given by $(E_0kT/2)^{\frac{1}{2}}$, where $E_0=2.45$ Mev is the mean neutron energy determined by the Q value of the reaction.

The observed standard deviations of Fig. 13 include a large "instrumental" contribution arising from the statistics and the resolution of the nuclear emulsion technique. This was determined independently from an exposure[25] with equal statistical uncertainty to *d-d* neutrons from a Cockcroft-Walton generator. The instrumental neutron width was found to be about 80 kev. Table II lists the observed standard deviations of Fig. 13 and also the standard deviations corrected for the instrumental width. The inferred ion temperature has a value in the neighborhood of 2 kev. However, in the case of the solid curves of Fig. 13, all of the neutron widths could be instrumental within the statistical uncertainty. This is in satisfactory agreement with the temperature determined from the proton and triton axial velocity distributions.

HARD X-RAY EMISSION

At deuterium pressures below 50 μ the emission of x rays whose energy is many times the voltage across the coil terminals is observed. These x rays arise primarily at the tube walls about 13 cm from the midplane of the coil, as shown by the darkening of film placed along the tube. The Pyrex tube used in early experiments was darkened in this region as if by electron bombardment.

The time distribution of x rays as well as neutrons is shown in Fig. 14. The asymmetric peak occurring just after the first field reversal is due to x rays, whereas the remaining peaks of decreasing amplitude centered on succeeding peak compressions represent neutrons. The deuterium pressure was 25 μ. A 3-mm lead shield surrounding the plastic scintillator removed the x-ray peak, and a crude absorption experiment using thin lead shielding showed that the maximum x-ray energy was at least 200 kev. For other operating conditions x-ray peaks were observed just before, as well as just after, magnetic field reversals.

These low-pressure x rays are attributed to electrons accelerated by the induced electric field in orbits described by a single-particle model and subsequently scattered out of the mirror to strike the tube walls some distance from the coil. With increasing deuterium pressure the hard x rays disappear, whereas the neutron yield increases as shown in Fig. 9. It was observed that impurities, which quenched the neutron yield, increased the x-ray yield. The absence of rf pre-excitation has the same effect.

The difference in time of occurrence of x rays and of neutrons, the difference in shape of the production-rate curves, and in general the contrasting behavior of the two radiations with regard to pressure, impurities, and rf excitation all tend to support the hypothesis that the mechanisms responsible for the x rays and the neutrons are quite different.

MAGNETIC PROBE STUDIES

Attempts to study the plasma by means of magnetic probes were found to be limited by the following difficulties: (a) the probes are either shattered or melted by the discharge, depending upon the material used, and (b) the presence of the probes in the region of the hot plasma severely affects the properties of the discharge itself. As a preliminary test of the perturbing effect of magnetic probes, a 2.0-mm diameter tungsten rod was placed parallel to the axis with its tip at various positions inside the Scylla coil. When the tip was at the center of the coil, the neutron yield was reduced to about 8% of its normal value. Actual probes jacketed with stainless steel, tantalum, or high alumina ceramic reduced the yield until it was not detectable above background. The most successful probes, capable of enduring as many as nine discharges, consisted of pickup coils cast into alumina jackets by means of epoxy resin. Those with electrostatic shields

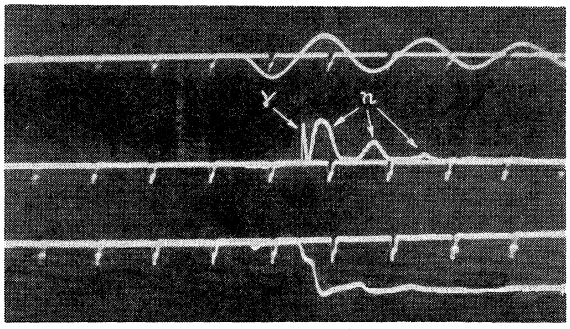

FIG. 14. The time distribution of hard x-ray emission and of neutrons (center trace) at a deuterium pressure of 25 μ with the applied magnetic field (upper trace). The time markers occur at 3-μsec intervals.

made of slotted hypodermic tubing had a diameter of 4.5 mm. Those without the shields, which were equally successful, had a diameter of 3.0 mm. Metal-jacketed probes were less durable and had the disadvantage that phase shifts were introduced into their signals because of the finite time required for the magnetic field to penetrate the metal jackets. In making the measurements, the probes were run into the discharge axially and were capable of both radial and axial adjustment so that the axial component of magnetic field at any position in the coil could be measured.

Figure 15 is a composite of magnetic probe signals and streak photographs adjusted to a common time scale. Figure 15(a) is an oscillogram in which the upper trace is the applied magnetic field and the lower trace is a typical magnetic probe signal with the probe centered in the plasma region. In Fig. 15(d), the magnetic probe signal is compared with the coil current in the absence of gas, showing that the probe signal faithfully records the magnetic field. With the magnetic probe inserted into the region of the fireball, Fig. 15(a) (lower trace), we observe the following phenomena: The magnetic field follows the vacuum or applied field during the first half-cycle, showing that the gas currents are small and have a negligible effect on the magnetic field. At the beginning of the second half-cycle the magnetic field is excluded for approximately 1 μsec, during which time however, a pip is observed whose sign is the same as that of the magnetic field in the preceding half-cycle. The time of occurrence of the pip corresponds closely to the time of arrival at the probe of the luminosity observed in the streak camera photograph [see Fig. 15(c)]. Near the current maximum of the second half-cycle the magnetic field indicated by the probe shows a sudden break and assumes the value of the driving field. In the third half-cycle the magnetic field of the second half-cycle is seen to be carried over until the sudden break occurs.

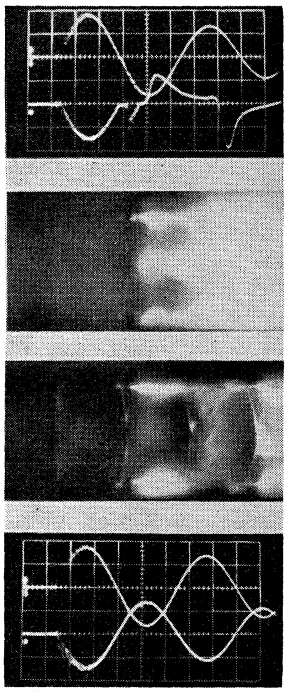

FIG. 15. (a) Magnetic probe signal (lower trace) with probe centered in the compression coil. The upper trace is the applied magnetic field. (b) Streak photograph of the radial motion of the light emitting portions of the plasma in the coil mid-plane with the probe centered in the coil. (c) Streak photograph with the probe removed from the compression coil. (d) Magnetic probe signal (lower trace) in the absence of gas with the applied field (upper trace).

The breakthrough seen by the probe is a matter of critical importance in the interpretation of the Scylla experiment, since it occurs at the time the neutron emission would have been a maximum in the absence of the probe, and the presence of this magnetic field would be totally incompatible with the existence of a ball of high-β, high-temperature plasma at this time. We have therefore to decide whether this sudden rise in the magnetic field is an artifact due to the presence of the probe when the neutrons are in fact absent or whether this magnetic field is in reality present even when there is no probe there to observe it.

Figure 15(b) is a streak photograph showing the radial motion of the light emitting portions of the plasma in the coil mid-plane. This photograph was taken simultaneously with Fig. 15(a). Figure 15(c) is a streak photograph taken with the probe retracted from the plasma region. A comparison of the streak photographs, Fig. 15(b) and Fig. 15(c), shows a large increase in the intensity of visible light emitted during the times of interest with the probe inserted. Figure 15(b) indicates that the probe injects impurities into the plasma. Intense visible light appears in the probe region as the compressed residual first half-cycle field approaches zero, 0.8 μsec after the beginning of the second half-cycle. No such light is observed in the absence of a probe, Fig. 15(c). This light emitting region rapidly grows to a diameter of at least 1 cm, or about two-thirds the diameter of the normal fireball. As the sudden break of the magnetic field occurs at the second half-cycle current maximum, the visible emission decreases appreciably and remains at a lower level throughout the duration of the break (0.3 μsec). As the magnetic field attains the driving field value, the visible emission increases and the region which it occupies expands radially. At the beginning of the third half-cycle, the discharge appears to be dominated by impurities.

It is believed that the observed probe signal is representative of the magnetic field which exists in the central plasma region up to the time of the break. The break is interpreted as being due to the rapid loss of plasma pressure due to cooling by impurities from the probe. The pip is a reproducible characteristic of the probe traces and is interpreted as due to the compression of a vestigial magnetic field from the first half-

cycle by an incoming shock. Much further progress has been made in probe studies to be deferred to other papers. We conclude that the break characteristic of signals with the magnetic probes immersed in the plasma is indeed an artifact not present when the probe is absent.

SUMMARY

The results of the foregoing experiments on a deuterium plasma, which was produced and heated in a rapidly rising axial magnetic field with a mirror geometry, show the following: (1) Essentially no hydromagnetic effects nor radiations are observed during the first half-cycle oscillation. (2) A strong radial "shock" occurs at the beginning of the second half-cycle with a velocity of 1.5×10^7 cm/sec. (3) Neutron emission from the $D(d,n)He^3$ reaction occurs on the second half-cycle and to a lesser extent on subsequent half-cycles with a symmetrical time distribution centered on the peak magnetic compressions. (4) The neutron emitting source has an ellipsoidal shape with a 1.5-cm diameter and a 2-cm axial length and is symmetrically located in the center of the compression coil. (5) The neutron yield increases with increasing residual deuterium pressure up to about 85 microns of Hg, decreases by approximately 50% and is relatively constant out to 250 microns as the pressure is increased further. (6) The neutron yield increases with increasing capacitor bank voltage in the range of 65 to 90 kv. (7) The *d-d* reaction rate decreases with the admixture of nitrogen impurity. (8) The neutron emission is isotropic with a narrow spread of energies in the radial direction. (9) The shape of the neutron emission time distribution is in good agreement with the theoretical shape predicted on the basis of initial "shock" heating followed by an adiabatic compression. (10) Wall impurities contaminate the discharge after the second half-cycle and increase the plasma resistance. (11) High-energy x-ray emission occurs at low deuterium pressures at times of maximum circumferential electric fields.

This paper reports the results of the experimental studies on Scylla from its inception up to the early months of 1959. Continuing studies with the same apparatus are reported in the papers which follow.

ACKNOWLEDGMENTS

The authors wish to express their appreciation to G. A. Sawyer and T. F. Stratton for their assistance in various diagnostic experiments and to T. M. Putnam and H. K. Jennings for aid in the design and construction of the various power supplies and control circuits. We are indebted to the Microscopy Group working under Louis Rosen for scanning and analyzing the nuclear emulsion data, to L. Cranberg for his help in the design and construction of the neutron collimator, and to R. B. Saunders, Jr., for the operation of the streak camera. We wish to thank F. L. Ribe for helpful discussions and assistance in the preparation of the manuscript. We also gratefully acknowledge the assistance of many other members of the Los Alamos Sherwood Project.

APPENDIX

The schematic diagram, Fig. 1, shows the method by which the ten 100-kv capacitors, C_1 to C_{10}, are connected through the spark gap switches, S_1 to S_{10}, to the compression coil. The gaps are individually mounted on their respective capacitors and are each connected with eight 4-meter lengths of *RG*-17/*U* cable to a common oil-immersed junction from which a short, tapering, parallel-plate transmission line leads to the compression coil. The parasitic inductance, as seen from the coil terminals, is 0.04 μh. The ten gaps are triggered within 0.04 μsec by direct cable connections, also 4 meters long, to the gap S_0 mounted on capacitor C_0. One of three dc bias voltages (+40 kv) on S_0 also serves to bias the central electrodes of the other gaps. The capacitors that are connected to the spark-point electrodes in the channel through the central electrodes consist of short lengths of stripped *RG*-17/*U* cable wrapped around the cylindrical metal housings of the 100-kv capacitors. The charging of these capacitors (capacitance $\sim$150 $\mu\mu$f) through the spark points serves to illuminate upper and lower gaps at the time of triggering. Triggering occurs when an input pulse from an ignitron and capacitor fires gap S_0, thus simultaneously changing the central electrode potential of the ten gaps from an initial +40 kv to −50 kv. A transient analysis of the triggering circuit shows that the small stray inductance of the triggering leads at each gap slightly delays, but increases the rate of potential change of the central electrode, in fact tending to make it overshoot the value −50 kv by a considerable amount. Each lower gap therefore is overvolted by several times its breakdown potential, and all lower gaps fire with negligible jitter. The potential of the central electrode now changes to +80 kv, and therefore each upper gap is overvolted more than fifty percent and is again highly illuminated by the spark-point electrode and the discharge in the lower gap. The upper gaps now fire, and all ten capacitors are thus connected to the compression coil. The 4-meter cable lengths electrically isolate the ten capacitors from each other for 0.04 μsec, so that a jitter in spark-gap firing approaching this amount can be accommodated. The extremely high reliability of the triggering system indicates that the actual gap firing jitter is always much less than 0.04 μsec.

It is worth noting that the result of one gap not firing with the others may lead to destruction of a 100-kv capacitor. If this gap fires after approximately one half-cycle of oscillation, a transient analysis of the normal modes of oscillation, neglecting damping, shows

that the potential on the capacitor whose gap has misfired may reach a maximum reversed potential approaching 2.6 times the initial potential to which it is charged.

The five-stage cascade charging circuit consists of five banks of seven 7.5-μf pyranol capacitors of 20-kv rating that are charged in parallel and discharged in series through a 50-μh inductance from which ten *RG*-17/*U* cables 10 m long lead to the individual 100-kv capacitors. Five four-element spark gap switches carry out the switching operation. The 100-kv capacitors are charged in 50 μsec to the potential 5.25 V_c, where V_c is the potential to which the cascade bank is charged. The capacitors in this bank are found to have a long life since they do not oscillate in potential. The charging inductor serves to isolate the cascade bank from the oscillating potential of the 100-kv capacitors during the operation of Scylla.

Note added in proof.—Reference to the work on axial magnetic field compression devices would not be complete without mention of recent work at the General Electric Research Laboratory[28] as well as that in Aachen, Germany,[29] in Fontenay-aux-Roses, France,[30] in Rome, Italy,[31] and in Sukhumi, U.S.S.R.[32]

[28] H. C. Pollock, L. M. Goldman, and F. Westendorp, Bull. Am. Phys. Soc. **5**, 367 (1960).
[29] H. Fay, E. Hintz, and H. L. Jordan, *4th International Conference on Ionization Phenomena in Gases, Uppsala, Sweden* (North-Holland Publishing Company, Amsterdam, 1960).
[30] M. Alidieres, R. Aymar, C. Etievant, P. Jourdan, P. Langer, and A. Samain, see footnote 29.
[31] J. E. Allen and S. Segre, see footnote 29.
[32] I. F. Kvartshava, K. N. Kervalidze, and J. S. Gvaladze, see footnote 29.

PHYSICAL REVIEW VOLUME 119, NUMBER 3 AUGUST 1, 1960

Continuum Radiation in the X Ray and Visible Regions from a Magnetically Compressed Plasma (Scylla)*

F. C. JAHODA, E. M. LITTLE, W. E. QUINN, G. A. SAWYER, AND T. F. STRATTON
Los Alamos Scientific Laboratory, University of California, Los Alamos, New Mexico
(Received March 28, 1960)

The identification of a sharp low-wavelength cutoff in the spectrum of x rays emitted from deuterium discharges in Scylla has resulted in the assignment of an electron temperature of 240±40 ev at the time of peak magnetic field compression. Simultaneous time-resolved absolute intensity determinations in the visible continuum, when coupled with the temperature measurement, yield an upper limit electron number density of $(5\pm1)\times10^{16}$/cm^3 at peak compression. The absolute value of $dE/d\lambda$ in the soft x ray region is two hundred times larger than bremsstrahlung from a pure deuterium plasma at the temperature and density quoted, and it is postulated that the large experimental $dE/d\lambda$ is the result of recombination radiation from about 2% of oxygen contaminant from the discharge tube walls.

I. INTRODUCTION

IT is possible, in principle, to determine many of the properties and characteristics of a plasma from an examination of the electromagnetic radiation emitted from the plasma itself. In particular, if the plasma temperature is greater than about 100 ev, the most characteristic radiation from pure deuterium is bremsstrahlung from electrons accelerated in the Coulomb field of the ions, and the electron temperature and density can be estimated from the spectrum shape and the total radiated power. If impurities are present, recombination and line radiation obscures the free-free radiation, particularly near the shorter wavelengths, and an interpretation of the experiment must be modified to include these processes. Spectral lines, where present, can be analyzed in terms of thermal or pressure broadening to yield information about the temperature and density, respectively. These techniques have been applied to the Scylla plasma compression experiment to measure the temperature, density, and purity of the deuterium discharge.

The Scylla experiment has been described previously.[1–3] In addition, detailed descriptions of other aspects of the apparatus and experimental results are presented in the articles preceding and following this account.[4,5] The data reported there show that the magnetic field compressing the plasma reaches 50 kilogauss in 1.25 μsec, and that about 3 cm^3 of volume is raised to a number density approaching 10^{17}/cm^3 and a deuteron temperature of 1.3 kev. In addition, at the time of neutron emission, soft x rays are detected

* Work performed under the auspices of the U. S. Atomic Energy Commission.

[1] W. C. Elmore, E. M. Little, and W. E. Quinn, Phys. Rev. Letters **1**, 32 (1958).
[2] W. C. Elmore, E. M. Little, and W. E. Quinn, (with K. Boyer), *Proceedings of the Second United Nations International Conference on the Peaceful Uses of Atomic Energy, Geneva, 1958* (United Nations, Geneva, 1958), Vol. 32, p. 337.
[3] D. E. Nagle, W. E. Quinn, W. B. Riesenfeld, and W. Leland, Phys. Rev. Letters **3**, 318 (1959).
[4] K. Boyer, W. C. Elmore, E. M. Little, W. E. Quinn, and J. L. Tuck, preceding paper [Phys. Rev. **119**, 831 (1960)].
[5] D. E. Nagle, W. E. Quinn, F. L. Ribe, and W. B. Riesenfeld, following paper [Phys. Rev. **119**, 857 (1960)].

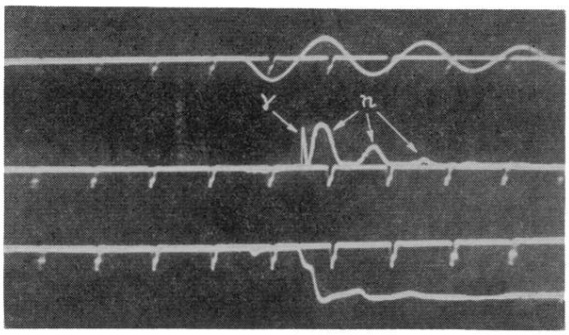

FIG. 14. The time distribution of hard x-ray emission and of neutrons (center trace) at a deuterium pressure of 25 μ with the applied magnetic field (upper trace). The time markers occur at 3-μsec intervals.

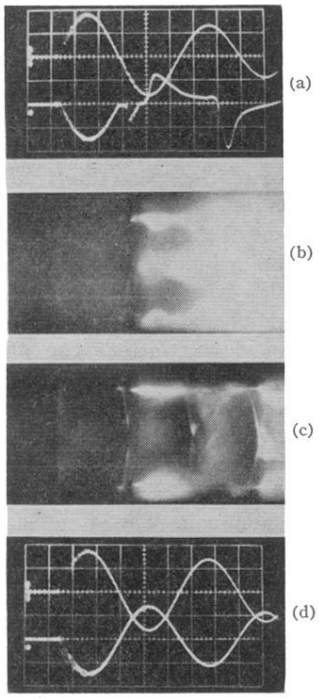

FIG. 15. (a) Magnetic probe signal (lower trace) with probe centered in the compression coil. The upper trace is the applied magnetic field. (b) Streak photograph of the radial motion of the light emitting portions of the plasma in the coil mid-plane with the probe centered in the coil. (c) Streak photograph with the probe removed from the compression coil. (d) Magnetic probe signal (lower trace) in the absence of gas with the applied field (upper trace).

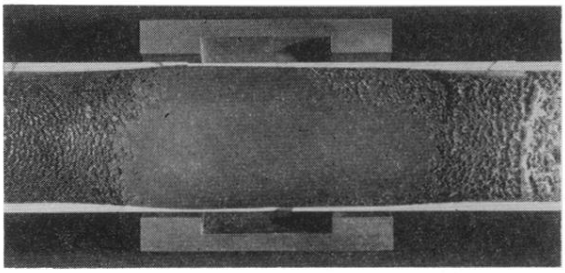

FIG. 3. Sections of 96% alumina tube after 3400 discharges and a Scylla coil.

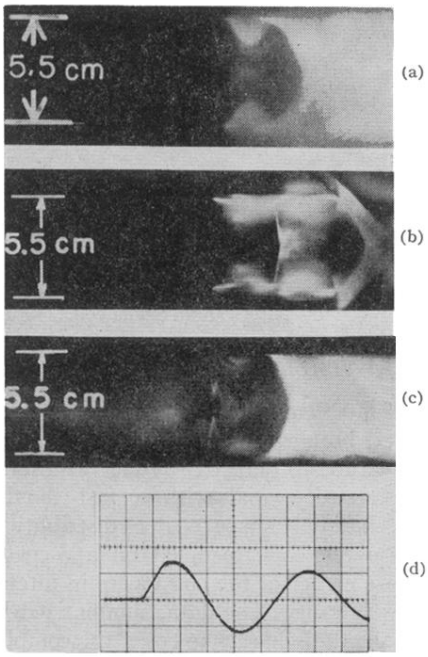

FIG. 5. Streak photographs of the radial motion of the light emitting portions of the plasma in the coil midplane. (a) and (b) Deuterium gas at a pressure of 90 μ with a capacitor bank voltage of 84 kv. (c) Helium gas at a pressure of 115 μ and a capacitor bank voltage of 84 kv. (d) Applied magnetic field which sets the time scale, 1 μsec per division.